MESOSTRUCTURAL APPROACH FOR CHARACTERISING MACROSCOPIC PARAMETERS OF OPEN CELL FOAMS WITH COMPUTED MICROTOMOGRAPHY

C. Perrot GAUS, Department of mechanical engineering, Université de Sherbrooke, Canada
R. Panneton GAUS, Department of mechanical engineering, Université de Sherbrooke, Canada
X. Olny ENTPE, DGCB URA CNRS 1652, Vaulx-en-Velin Cedex, France
R. Bouchard GAUS, Department of mechanical engineering, Université de Sherbrooke, Canada

1 INTRODUCTION

This paper presents recent research activities at the University of Sherbrooke in the characterization of open-cell foams from the cell's morphology. The goal is to link the morphology to the most common macrospic acoustic parameters (porosity, resistivity, tortuosity, characteristic lengths and thermal permeability); and to link the acoustics to material sciences (see figure 1) in view of guiding the design of acoustical foams. To achieve this, one needs first to determine the local geometry of the media. The use of the modern technique of Computed Micro Tomography (CMT) is investigated. Difficulties met until now, and proposed solutions will be presented. In a first attempt, only the scalar macroscopic parameters (porosity and thermal characteristic length) are investigated. Let us mention that microstructural approaches have originally been initiated in the field of mechanical properties. Similar approaches in the field of transport properties rely on the reconstruction of the porous media by some statistical techniques.

2 MACROSCOPIC PARAMETERS OF FOAMS (ACOUSTICS)

In acoustics, open-cell porous foams used in sound absorbing applications are classically characterized by macroscopic parameters. The most common of these parameters are the porosity, static airflow resistivity, tortuosity, viscous characteristic length, thermal characteristic length, and thermal permeability. These parameters are confidently used in models to predict the acoustical behavior of these materials [1-3]. Typically, under the assumption of a rigid frame, the different sources of dissipation are separated (visco-inertial and thermal), and the exact asymptotic behavior of the macroscopic laws governing these processes is derived. Mathematical parameters involved in these formulations are finally related to the measurable macroscopic parameters.

The characterization of these parameters is done at a macroscopic scale (i.e. homogeneous properties) using different methods. While porosity, resistivity, and tortuosity (for non conductive frame) can be directly measured [4-6], the other parameters are usually measured using acoustical methods [7,8]. However, all of these methods give no clue on the morphology of the cells and no interrelation between the macroscopic parameters. This limits the guided design of acoustical foams since the manufacturer mostly control the morphological parameters of the foams (density, cell topology and geometry).

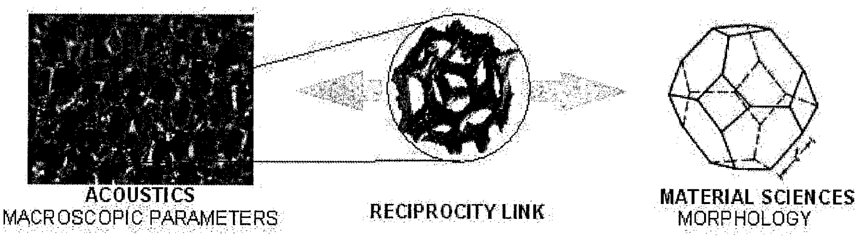

Figure 1: Linking acoustics to material sciences

In the following, since only the two scalar geometrical macroscopic parameters of the foams will be investigated, their mathematical descriptions are now introduced. These parameters are the open porosity and thermal characteristic length. They are scalar geometrical properties since they only depend on the geometry of the porous network. The porosity is given by:

$$\Phi = V/V_b \ , \qquad \text{(Eq. 1)}$$

where V is the volume of the open air space contained in a macroscopic bulk volume V_b of the foam. Similarly, the characteristic lengths is given by

$$\Lambda' = 2\int_V dV \Big/ \int_A dA \, . \qquad \text{(Eq. 2)}$$

The integrations in the numerator and denominator are over the volume V and surface A of the pores, respectively.

3 MORPHOLOGICAL PARAMETERS OF FOAMS (MATERIAL SCIENCES)

In the previous section, it was mentioned that the acoustics of foams is based on macroscopic measurements. We shall now introduce the cell's morphology that is used in this study to develop the reciprocity link between the macroscopic parameters and the cell's morphology. Different morphologies of cells could have been chosen. However, to respect some physical considerations in the creation of foams and the simplicity of the proposed model, the tetrakaidecaedral unit cell was chosen[9], see figure 2. Discussion of this choice is beyond the scope of this paper. However, one can note that this topology fairly represents real foam's cell (see figure 5).

The tetrakaidecaedral unit cell is a periodical structuring element, which can be seen as the mesostructural bridge linking scalar macroscopic parameters (acoustics) and microscopic descriptors (material sciences). It is an idealized model of high porosity open cell foam, and a good approximation of the surface area covered by a real foam's cell.

From this mesostructure, it is shown that the couple of scalar macroscopic parameters (Φ, Λ') can be entirely defined by a corresponding couple of microstructural descriptors (l, d); where l and d define the length and diameter of the cell's struts, respectively. Assuming (i) a circular cross section of the struts (edges), and a strut's length much larger than the strut's diameter (i.e. high porosity foam), Gibson and Ashby have given the theoretical porosity associated to such a unit cell[10], see Table 2. Similarly, we have prolonged their calculations to obtain the analytical expressions of the thermal characteristic length associated with various kinds of cross sectional shape areas. Only the results are presented in Table 2.

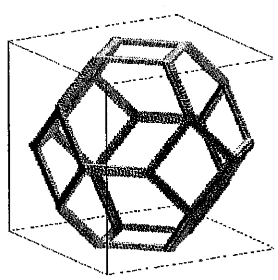

Figure 2: Regular tetrakaidecahedron unit cell

Table 1: Analytical macro-micro relationships

Assumption on the shape of the cross sectional area	Porosity ? (Eq. 3a,b)	Thermal characteristic length ?' (Eq. 4a,b)
Circular d, diameter l, length	$1-\frac{3\pi}{8\sqrt{2}}\left(\frac{d}{l}\right)^2 \approx 1-0.83\left(\frac{d}{l}\right)^2$	$\frac{4\sqrt{2}}{3\pi}\frac{l^2}{d}-\frac{d}{2}=\frac{d}{2}\left(\frac{\Phi}{1-\Phi}\right)\approx 0.60\frac{l^2}{d}-0.5\,d \approx 0.5\left(\frac{\Phi}{1-\Phi}\right)$
Triangular b basis h height l, length	$1-\frac{3\sqrt{3}}{8\sqrt{2}}\left(\frac{b}{l}\right)^2 \approx 1-0.46\left(\frac{b}{l}\right)^2$ $1-\frac{\sqrt{3}}{2\sqrt{2}}\left(\frac{h}{l}\right)^2 \approx 1-0.61\left(\frac{h}{l}\right)^2$	$\frac{4\sqrt{2}}{9}\cdot\frac{l^2}{b}-\frac{b}{2\sqrt{3}}=\frac{b}{2\sqrt{3}}\left(\frac{\Phi}{1-\Phi}\right)\approx 0.63\frac{l^2}{b}-0.29b \approx 0.29\left(\frac{\Phi}{1-\Phi}\right)$ $\frac{2\sqrt{2}}{3\sqrt{3}}\cdot\frac{l^2}{h}-\frac{h}{3}=\frac{h}{3}\left(\frac{\Phi}{1-\Phi}\right)\approx 0.54\frac{l^2}{h}-0.33b \approx 0.33\left(\frac{\Phi}{1-\Phi}\right)$

4 COMPUTED MICROTOMOGRAPHY

To use the equations presented in the previous sections, one need real three-dimensional local information. In this study, this information is obtained by means of computed microtomography (µCT). The system used is a Skyscan desktop µCT scanner presented in figure 3. This µCT is based on the same physical principles and mathematical algorithms as the classical medical CT-scanners. During the data acquisition, the µCT scanner collects 2-dimensional X-ray images through the object from different views through 180-degres object rotation (see figure 3b). Corresponding lines from all views are used afterwards in the reconstruction procedure to create a 3D image by a tomographical back projection algorithm (see figure 3c). Note that the main technical improvements compared to the medical scanners which were operating in the sixties, is the use of a microfocus X-ray tube with a higher energy sealed tube (for penetrating harder materials), and a modern detector (a CCD camera instead of a photographic plate).

Calibration of the three-dimensional µCT image

At first, nothing guarantees the fidelity of a 3D image produced by µCT to the original real object. Many artefacts have to be filtered and image processing have to be done in view to obtain a good visual quality of the 3D image. Despite all of the filtering and processing, the quality of the 3D image limits the fine measurement of the dimensions of the different features of the tomograhied object. In this study, to improve the fidelity of the 3D image and the precision in the measurement of the microstructural descriptors l and d, a calibration test on the 3D image is proposed.

The calibration test consists in comparing the computed open porosity obtained by image processing on the 3D image to the one directly measured using classical techniques. Here the computed open porosity is obtained using eq.1 and an image processing in which the volume V of air (black region) and the bulk volume V_b of the 3D image are determined. As an example, figure 4 shows a 3D image obtained for an aluminium foam. Prior to the calibration, one can observed solid particles hanging in the air phase (the air phase is coloured in black in the image). These particles are artefacts and are non real. They decrease the computed open porosity of the foam. During the calibration, the contrast is adjusted so that the computed open porosity equals the one directly measured. This calibration reduces significantly the non-physical effects of artefacts that may be produced by the µCT system, and yields a cleaned image, as shown in figure 4 .

a) The experimental set-up

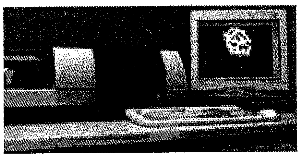

Skyscan 1072 desktop μCT scanner

b) The main parts of the setup

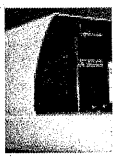

Microfocus x-ray

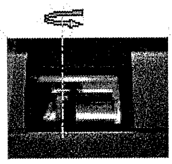

Rotating sample holder

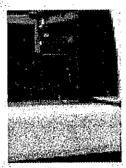

CCD camera

c) μCT advantages

Digital radiography system
- produces 2D images
- no in-depth information

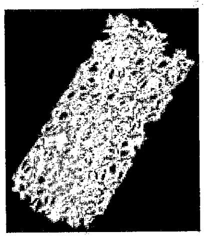

μCT system
- produces 3D images
- internal structure information

Figure 3: Experimental set-up and results

Measurement protocol

Finally, once a three-dimensional calibrated image is acquired, microstructural measurements are carried out through a visualization and measurement tool specifically developed for this study under the Matlab™ environment. With this tool, isolated cells are analyzed according to the following measurement protocol. First, a reference plane is positioned so that it passes through a window belonging to the studied cell. Second, the length l and depth d of each of the struts forming the contour of the window are measured. The internal perimeter of the window is also reported, as well as the radius R of a circle inscribed in the window. Next, the first and second steps are repeated until all the windows of a cell are analyzed. To close the measurement protocol for one cell, the radius of a sphere inscribed in the cell is estimated. Following this protocol, since a strut is shared between two windows for an isolated cell, each of the strut dimensions has been measured twice. This improves the validity of the measurements.

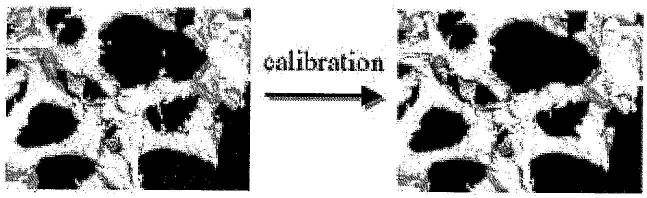

Figure 4: Calibration of the three dimensional CMT image

5 APPLICATION FOR DUOCEL© 40 PPI ALUMINIUM FOAM

Investigations have been carried out for a Duocel aluminium foam sample (40 pores per inch). The sample measures 5 mm in diameter and around 40 mm in height. It has been scanned at the lowest magnification of the desktop. The magnification factor is 10. The corresponding resolution is 21.80 micrometers per pixel.

Using the classical macroscopic techniques discussed in section 2, the measurements of the macroscopic open porosity and thermal c haracteristic yield, respectively:

$$\Phi = 0.920$$
$$\Lambda'(\mathrm{mm}) = 1.484 \pm 0.154$$

Following the microscopic approach and the measurement protocol described in section 4, the values of the microscopic parameters measured on a single cell are:

$$\langle l \rangle = 1.11 \pm 0.37 \text{ mm}$$
$$\langle d \rangle = 0.37 \pm 0.15 \text{ mm}$$
$$\langle R \rangle = 1.37 \pm 0.05 \text{ mm}$$

Figure 5 also recalls the definition of the macroscopic parameters *l, d,* and *R*.

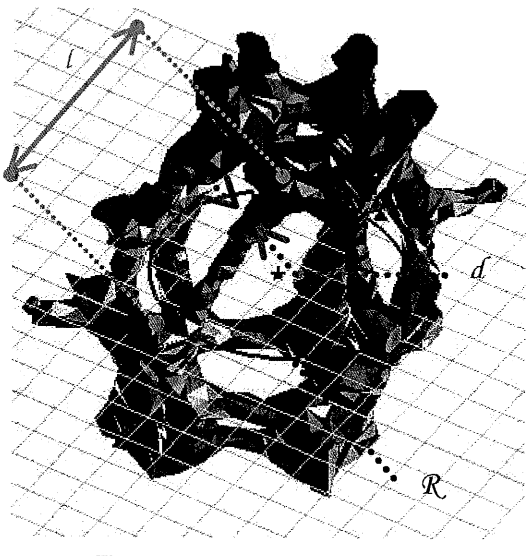

Figure 5: Microscopic parameters

Micro to macro

Using these values in the theoretical micro-macro relationships given by eqs. 3a and 4a, the open porosity and thermal length are:

$$\Phi = 0.864 \ (5.6\ \%)$$
$$\Lambda'(\mathrm{mm}) = 1.451 \ (2.19\ \%)$$

where the percentages in parenthesis are the relative errors compared with the macroscopically measured values. The theoretical predictions are based only on the characterization of a single cell taken randomly. To minimize the relative error, the analysis must be performed on many cells. The number of cells required, so that the errors tend to zero, is linked to the macroscopic volume of homogenisation or the Representative Volume Element (RVE). For high porosity foams, this RVE has yet to be defined (this is beyond the scope of this paper).

Since it is possible to predict some macroscopic features of the foam morphology with microscopic information averaged only on a single cell, one can conclude that local information can be used to predict global information.

Macro to micro

In a same manner, using the macroscopically measured parameters in the micro-macro relationships given by eqs. 3a and 4a, the microscopic parameters can be deduced. They are given below with their relative errors compared to the one measured on the single cell:

$$\langle l \rangle = 0.83 \text{ mm } (44\ \%)$$
$$\langle d \rangle = 0.26 \text{ mm } (30\ \%)$$
$$\langle R \rangle = 1.17 \text{ mm } (15\ \%)$$

These results show that the reverse relationships (macro to micro) yield larger errors than the direct relationships (micro to macro). This is logical since the direct relationships show squared small numbers, and the reverse relationships show roots of larger numbers. In the reverse case, the predictions of the microscopic parameters should be compared to the microscopic parameters measured following the proposed protocol and averaged over many cells or, in other words, over the RVE.

6 CONCLUSION AND PERSPECTIVES

This study proposed a calibration test and a measurement procedure to obtain from computed microtomographic (µCT) analyses acceptable precision in the characterization of the microstructural topology of open foams. It was shown that the tetrakaidecahedron unit cell topology permits to establish theoretical reciprocity links between scalar macroscopic parameters (acoustics) and microstructural indicators (material sciences). An application to an aluminum foam showed that, from the knowledge of the microscopic parameters of single cell chosen randomly, the reciprocity links yield small errors in the prediction of the macroscopic parameters (porosity and thermal characteristic length). However, the prediction of the microscopic parameters of this single cell from the macroscopic parameters yield large errors. To minimize the errors, it was pointed out that the analysis must be performed on the number of cells contained in a representative volume element (RVE). The determination of the RVE for acoustical foams is still an open question. The proposed procedure could be used confidently to establish the minimum number of cells required for the RVE.

7 ACKNOLEDGEMENTS

The authors wish to thank ALCAN, NSERC, FQRNT, and CQRDA for their financial support to the project.

8 REFERENCES

1. D. Lafarge, P. Lemarinier, J.F. Allard, and V. Tarnow, 'Dynamic compressibility of air in porous structures at audible frequencies', J. Acoust. Soc. Am. 102(4) 1995-2006. (1997).
2. J.F. Allard. Propagation of sound in porous media, London and New York: Elsevier Applied Science. (1993).
3. D.K. Wilson, 'Relaxation-matched modeling of propagation through porous media, including fractal pore structure', J. Acoust. Soc. Am. 94(2) 1136-1145. (1993).
4. Y. Champoux, M.R. Stinson, and G.A. Daigle, 'Air-based system for the measurement of the porosity', J. Acoust Soc. Am. 89, 910-916 (1990).
5. J.F. Allard, B. Castagnède, M. Henry, and W. Lauriks, 'Evaluation of tortuosity in acoustic porous materials saturated by air', Rev. Sci. Instrum. 65, 754-755 (1994).
6. M. R. Stinson and G. A. Daigle, "Electronic system for the measurement of flow resistance," J. Acoust. Soc. Am. 83, 2422-2428 (1988).
7. P. Leclaire, L. Kelders, W. Lauriks, M. Melon, N. R.Brown, and B. Castagnede, 'Determination of the viscous and thermal characteristic lengths of plastic foams by ultrasonic measurements in helium and air', J. Appl. Phys. 80, 2009-2012 (1996).
8. Y. Atalla and R. Panneton, 'Three parameters inverse characterization of open cell porous media through impedance tube measurements', accepted for publication in J. Acoust. Soc. Am. (2002).
9. N.C. Hilyard and A. Cunningham: Low density cellular plastics, Chapman & Hall, London. (1994).
10. L.J. Gibson and M.F. Ashby: Cellular solids, structure and properties, 2nd ed., Cambridge University Press, Cambridge. (1997).